

DOI: 10.1002/elan.201700806

# Electrochemical Detection of Acetaminophen with Silicon Nanowires

Raja Ram Pandey,<sup>[a]</sup> Hussain S. Alshahrani,<sup>[a]</sup> Sergiy Krylyuk,<sup>[b, c]</sup> Elissa H. Williams,<sup>[c]</sup> Albert V. Davydov,<sup>[c]</sup> and Charles C. Chusuei<sup>\*[a]</sup>

**Abstract:** Acetaminophen (APAP) is an antipyretic, analgesic agent, the overdose of which during medical treatment poses a risk for liver failure. Hence, it is important to develop methods to monitor physiological APAP levels to avoid poisoning. Here, we report an efficient, selective electrochemical APAP sensor made from depositing silicon nanowires (SiNWs) onto glassy carbon electrodes (GCEs). Electrocatalytic activity of the SiNW/GCE sensors was monitored under varying pH and concentrations of APAP using cyclic voltammetry (CV)

and chronoamperometry (CA). CV of the SiNWs at 0.5 to 13 mmol dm<sup>-3</sup> APAP concentrations was used to determine the oxidation and reduction potentials of APAP. The selective detection of APAP was then demonstrated using CA at +0.568 V vs Ag/AgCl, where APAP is fully oxidized, in the 0.01 to 3 mmol dm<sup>-3</sup> concentration range with potentially-interfering analytes. The SiNW sensor has the ability to detect APAP well within the detection limits for APAP toxicity, showing promise as a practical biosensor.

**Keywords:** silicon nanowires • acetaminophen • toxicity monitoring • biosensor

## 1 Introduction

Acetaminophen (APAP), an antipyretic, analgesic agent, is one of the most commonly found pharmaceuticals in the household [1] and among the most frequently identified contaminants in sewage and surface water [2–5]. Liver failure due to APAP overdose is common in developed countries [6]. According to the Rumack-Matthew nomogram, APAP concentrations greater than 150 µg/mL (equivalent to 1 mmol dm<sup>-3</sup>) are toxic [7]. For this reason, practical clinical methods for monitoring APAP are necessary to ensure proper dosages and prevent organ injury. Analytical methods, such as liquid chromatography, high performance liquid chromatography, spectrophotometry, and electrospray mass spectrometry have been used for the analysis of APAP in pharmaceutical formulas and biological fluids [8]. Unfortunately, these analytical techniques are limited due to their relatively complex operational procedures and high cost. On the other hand, electrochemical methods such as cyclic voltammetry (CV) and chronoamperometry (CA) are simple, rapid, relatively inexpensive [9], and applicable for studying electroactive compounds, including APAP, in physiological fluids.

Silicon nanowires (SiNWs) are among the most sought after nanomaterials for their role in sensing technologies and catalytic reactions [10,11]. The main advantages of silicon nanowires (SiNWs) over other 1D electrocatalyst materials (e.g., carbon nanotubes) include high crystallinity and the ability to tune conductivity by doping. Chemical vapor deposition (CVD) provides a controllable method to produce SiNWs with varying diameters and lengths [12]. SiNW surfaces permit easy functionalization with molecular targets that can bind to specific analytes of

interest [13]. Having a high aspect ratio (~10<sup>3</sup>) at the nanoscale means that SiNWs can be applied to monitor complex regulatory and signaling patterns of inner cells [14]. In addition, they are biocompatible, non-toxic, and sensitive for the identification of biomolecules [15]. Lieber et al. showed the applicability of SiNW field-effect transistors for the detection of Ca<sup>2+</sup>, H<sup>+</sup>, and bovine immunoglobulin (IgG) [16]. Li and co-workers [17] reported the utility of SiNWs as DNA sensors. Recently, SiNWs have been used as a means of sensing metal ions in solution [18] and antigen dissociation [19].

In this study, we report electrochemically active SiNWs for the quantitative, selective detection of APAP in aqueous solution employing SiNW-modified glassy carbon electrodes (GCEs). To the best of our knowledge, this is the first report of a SiNW-based sensor to quantify APAP under physiological pH conditions.

[a] R. R. Pandey, H. S. Alshahrani, C. C. Chusuei  
Chemistry Department, Middle Tennessee State University  
Murfreesboro, 440 Friendship Street, TN 37132  
E-mail: Charles.Chusuei@mtsu.edu

[b] S. Krylyuk  
Theiss Research, La Jolla, CA 92037

[c] S. Krylyuk, E. H. Williams, A. V. Davydov  
Materials Science and Engineering Division, Material Measurement Laboratory, National Institute of Standards and Technology, Gaithersburg, MD 20899

Supporting information for this article is available on the WWW under <https://doi.org/10.1002/elan.201700806>

## 2 Experimental

### 2.1 Material Preparation

Au-catalyzed silicon nanowires (SiNWs), ca. 30 nm in diam and 14  $\mu\text{m}$  in length, were grown in a custom-built CVD system operated at 900 °C and 80 kPa reactor pressure using a  $\text{SiCl}_4/\text{H}_2/\text{N}_2$  gas mixture. Catalytic growth was initiated using 30 nm diam Au nanoparticles randomly dispersed on Si(111) substrates functionalized with poly-L-lysine, the procedure of which is fully described elsewhere [12]. SiNWs were released from the substrate by sonication in 2 mL of reagent grade isopropanol purchased from Fisher Scientific (Fair Lawn, NJ, USA) for 2 min. The suspended SiNWs were then used to modify the GCEs (5 mm diam, Pine Research Instrument Co., Raleigh, NC, USA).

### 2.2 Electrode Preparation

Prior to modification, the GCE was polished using a 1.0- $\mu\text{m}$  diameter  $\text{Al}_2\text{O}_3$  slurry, rinsed with  $\text{H}_2\text{O}$ , and then polished further using a 0.05- $\mu\text{m}$  diameter  $\text{Al}_2\text{O}_3$  slurry to a mirror-like finish. Both slurries were obtained from Buehler, Ltd (Lake Bluff, IL, USA). Millipore (Milli-Q water filtration system, Model Elix, USA) deionized water was used in all experiments. GCEs were then cleaned by sonication in a 1:1 mixture (by volume) of concentrated  $\text{HNO}_3:\text{H}_2\text{O}$  followed by water rinse and drying in air. Aliquots of 10  $\mu\text{L}$  containing SiNWs suspended in isopropanol was deposited on the surface of a freshly polished GCE, followed by drying in air. The SiNWs were then encapsulated on GCEs by applying a 10- $\mu\text{L}$  aliquot of Nafion (2 wt%) in absolute anhydrous ethanol (Pharmaco-AAPER, Brookfield, CT, USA), followed by drying in an oven at 80 °C. Additional aliquots of the SiNW colloid were applied to the GCE and dried as needed. The resulting Nafion/SiNW/GCE structures were used as working electrodes.

### 2.3 Characterization

A scanning electron microscopy (SEM) image of the SiNWs having the best APAP detection characteristics is shown in the Supporting Information (Figure S1, ESI). EDX, ATR-IR, and XPS were also used to characterize the SiNWs (Figures S2–S4, ESI). SEM analysis showed that the optimum SiNW coverage resulting in maximum signal response for APAP detection was  $(1.4 \pm 0.5) \times 10^3$  SiNWs/ $\text{mm}^2$  ( $n=53$ ). This SiNW surface density was obtained by depositing two consecutive colloidal aliquots (a total volume of 20  $\mu\text{L}$ ), allowing for drying between applications. This optimum loading of 20  $\mu\text{L}$  on the GCE provides the highest current (Figure S5, ESI).

Electrochemical activity of the SiNWs was studied using cyclic voltammetry (CV) and chronoamperometry (CA). Experiments were conducted using AfterMath™ software (ver 1.2.5658) and a WaveNano potentiostat (Pine Research Instrument Co., Raleigh, NC, USA). A

custom-built Faraday cage constructed of a copper (Cu) grid mesh was used to reduce external electromagnetic interference. The three-electrode electrochemical cell consisted of a Ag/AgCl (3.5 mol  $\text{dm}^{-3}$  KCl) reference electrode, a counter electrode made of platinum wire, and a Nafion/SiNW/GCE working electrode stored in inert  $\text{N}_2$  atmosphere until usage. CVs of the cell were studied in the range of potentials from  $-1.0$  V to  $+1.0$  V using a  $50$   $\text{mV s}^{-1}$  scan rate. The optimum peak potential based on maximum height in the CVs for APAP detection was selected for CA analysis. APAP concentrations of 0.5 to 13  $\text{mmol dm}^{-3}$  were used since these concentrations are well within clinical monitoring purposes [7,8]. Phosphate buffer solution (PBS) was used as the medium to adjust the pH of the electrochemical cell. All chemical reagents were of 99.9% purity or greater and obtained from Sigma-Aldrich (St. Louis, MO, USA). All experiments were performed in deoxygenated electrolyte solution prepared by bubbling 99.9% purity  $\text{N}_2$  gas flow (Air Gas Products, Radnor, PA, USA) through the solution for 15 min prior to each measurement.

(Disclaimer: Certain commercial equipment, instruments, or materials are identified in this paper in order to specify the experimental procedure adequately. Such identification is not intended to imply recommendation or endorsement by the National Institute of Standards and Technology, nor is it intended to imply that the materials or equipment identified are necessarily the best available for this purpose.)

## 3 Results and Discussion

Figure 1 shows CVs of (a) Nafion/SiNW/GCE and (b) bare GCE in a 10 mM APAP solution at pH=7.4. Well-defined reduction and oxidation peaks at  $-0.058$  V and

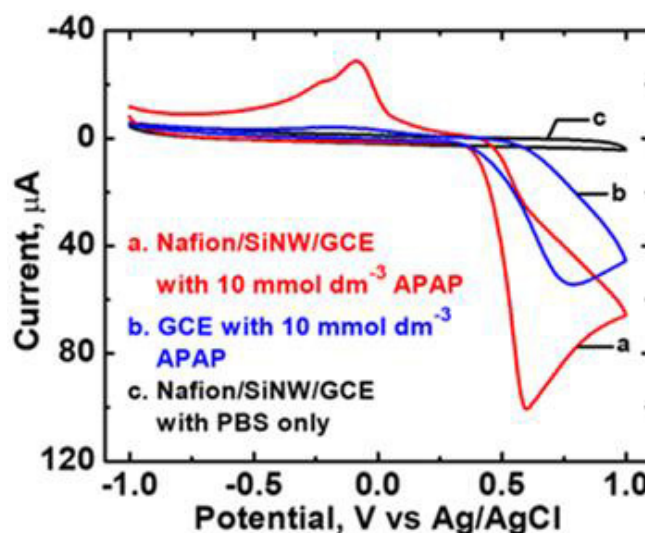
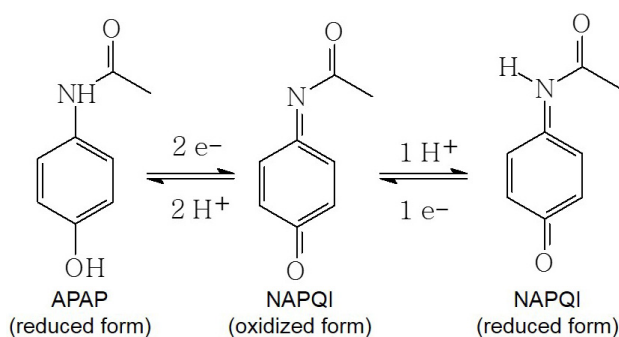


Fig. 1. CV of bare and modified GCE in pH=7.4 phosphate buffer at a scan rate of  $50$   $\text{mV s}^{-1}$ : (a) SiNW/GCE, (b) bare GCE in  $10$   $\text{mmol dm}^{-3}$  APAP, and (c) SiNW/GCE in PBS only.

+0.568 V vs Ag/AgCl, respectively, are observed in the CV using the Nafion/SiNW/GCE. Peak currents using the Nafion/SiNW/GCE (Figure 1a) are considerably higher as compared to that of the bare GCE (Figure 1b). The increase is attributed to the increase in electroactive surface area in the SiNW/GCE. Asymmetric peak shapes in the CVs at various pH conditions (*vide infra*) denoted irreversible redox processes. During CV, APAP is oxidized to N-acetyl-p-benzoquinone imine (NAPQI) and NAPQI is reduced back to APAP via a two-electron process. A very small amount of NAPQI also undergoes reduction (Scheme 1), resulting in a smaller peak in reduction potential at a 10 mmol dm<sup>-3</sup> concentration of APAP at -0.223 V (Figure 1) [20]. Nafion/SiNW/GCE in the blank phosphate buffer solution (PBS) at pH=7.4 showed no signal (Figure 1c).



Scheme 1. Forms of APAP and NAPQI.

Figure 2 shows the amperometric response of the Nafion/SiNW/GCE as a function of pH at APAP's determined reduction and oxidation potentials of -0.058 V and +0.568 V, respectively; the corresponding CVs of 10 mmol dm<sup>-3</sup> APAP are shown in the Supporting Information (Figure S6, ESI). The cathodic peak current showed no response from pH=2.0 to 5.0; the anodic current decreased in this range. Cathodic and anodic currents increased from pH=6.0 to 8.0; current then decreased at pH values higher than 8.0. Maximum current was observed at pH=8.0 for both oxidation and reduction potentials. Since pH=7.4 more closely resembles physiological conditions and is near the highest reactivity, we focus the remainder of our studies at this pH value.

Randles-Sevcik analysis, showing a linear relationship of current as a function of the square root of the scan rate, reveals that both oxidation and reduction of APAP at the Nafion/SiNW/GCE surface is diffusion controlled, owing to the spontaneous mass transport of electroactive species from regions of higher concentration to the regions of lower concentrations. This phenomenon is characterized by the peak currents of reduction ( $I_{pc}$ ) and oxidation ( $I_{pa}$ ) to scale proportionally with the square root of the scan rate for irreversible redox processes according to the equation [21,22]:

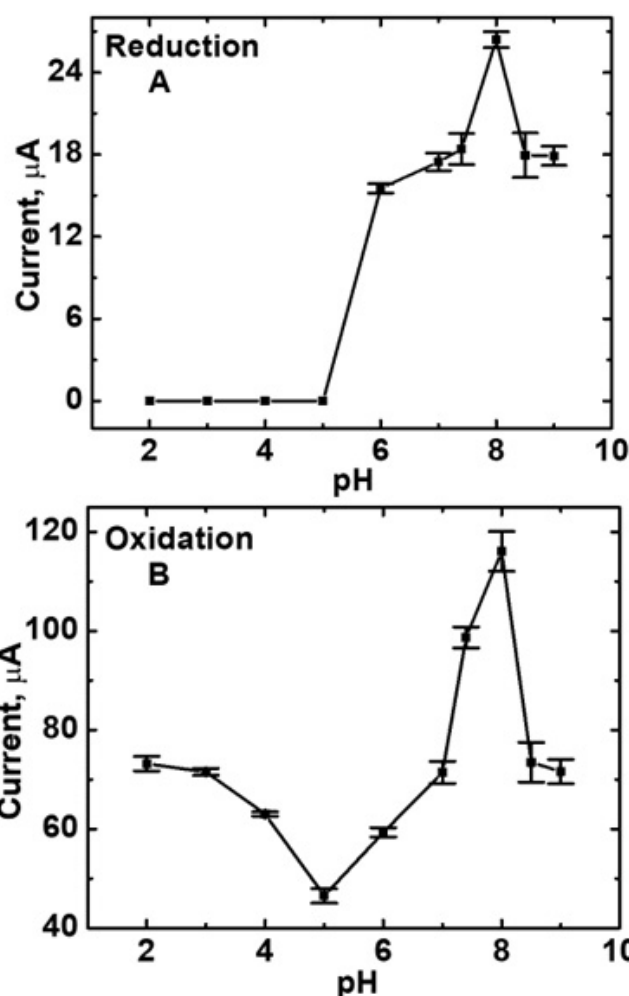


Fig. 2. Peak current of 10 mmol dm<sup>-3</sup> APAP of Nafion/SiNW/GCE as a function of pH in different phosphate buffer solutions with a sweep rate of 50 mV s<sup>-1</sup> at (A) reduction and (B) oxidation potentials.

$$I_p = 0.4961 \text{ nFAC}_A^* \left( \frac{anFvD_E}{RT} \right)^{1/2} \quad (1)$$

where  $I_p$  is the peak current in A,  $a$  is the transfer coefficient,  $n$  is the number of electrons,  $A$  is the electrode area (cm<sup>2</sup>),  $D_E$  is the diffusion coefficient at the electrode surface (cm<sup>2</sup>s<sup>-1</sup>),  $C_A^*$  is the concentration in mol cm<sup>-3</sup>, and  $v$  is the scan rate in Vs<sup>-1</sup>,  $R$  is the universal gas constant,  $n$  is the number of electrons involved in the redox reaction,  $F$  is the Faraday constant, and  $T$  is the absolute temperature. Figure 3A demonstrates the scan rate dependence on the peak current. For both APAP reduction and oxidation, a linear correlation of peak currents and  $v^{1/2}$  is observed, as shown in Figures 3B and 3C, respectively. The corresponding curvefitted equations for  $I_{pc}$  and  $I_{pa}$  are:

$$I_{pc} (\mu\text{A}) = 1.405v^{1/2} (\text{V s}^{-1}) + 1.118 \quad (R^2 = 0.9806) \quad (2)$$

$$I_{pa} (\mu\text{A}) = 4.293v^{1/2} (\text{V s}^{-1}) + 16.998 \quad (R^2 = 0.9868) \quad (3)$$

Equation (1) was used to estimate charged molecule diffusion coefficients for redox processes. Diffusion coefficient calculations were made based on multiple CV measurements are summarized in the Supporting Informa-

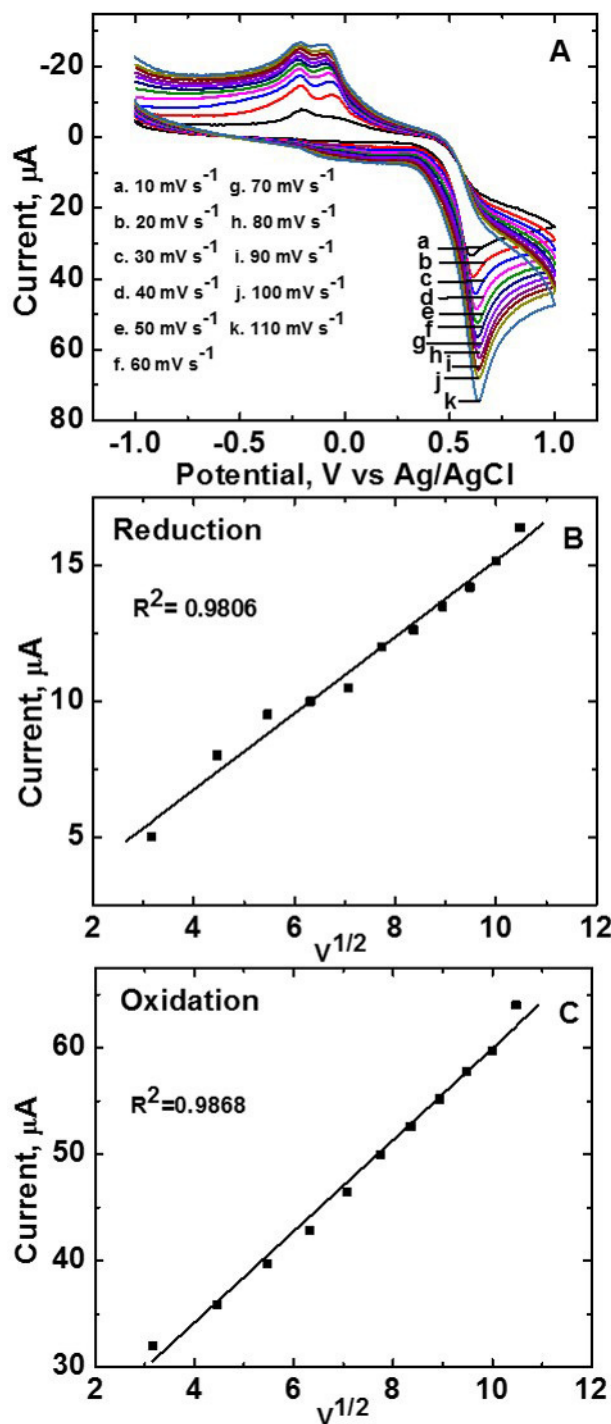


Fig. 3. (A) CV of  $10 \text{ mmol dm}^{-3}$  APAP at  $\text{pH}=7.4$  on Nafion/SiNW/GCE at the scan rates indicated in the figure; (B) plot of  $I_{pc}$  vs  $v^{1/2}$  at reduction (B); and oxidation (C) potentials.

tion [Table S1 (MS Excel spreadsheet with embedded formulae), ESI]. Assuming the limiting case in which the transfer coefficients for reduction and oxidation processes are equal, the  $\alpha D_E$  constants for the reduction and oxidation processes were found to be  $(9 \pm 1) \times 10^{-7} \text{ cm}^2 \text{ s}^{-1}$ , and  $(1.8 \pm 0.7) \times 10^{-5} \text{ cm}^2 \text{ s}^{-1}$ , respectively ( $n=11$ ), applying the xy data points in Figure 3A and solving for  $\alpha D_E$  in Equation 1. These values are well within calculated diffusion coefficients for APAP in solution [23]. Numerical values for  $\alpha D_E$  indicate faster diffusion for oxidation than reduction, consistent with the observed higher oxidation current (Figure 3A). There is a 20-fold greater sensitivity to oxidation as compared to reduction. This phenomenon in part is attributed to Coulombic attraction between the APAP and SiNW electrode surface driving greater diffusion during oxidation as compared to reduction. The isoelectric point of APAP as measured by the  $\text{pK}_a$  value is 9.7 [23]; hence, under  $\text{pH} 7.4$  conditions, the protonated form of APAP is dominant and is positively charged. SiNWs are known to have a PZC of 2.9 [24], and therefore adopts a negative charge at this solution pH. Le Châtelier's principle also plays a role contributing to the enhanced oxidation. Since the concentration of the protonated form of APAP in the bulk solution is significantly large, oxidation will dominate (over reduction) on the GCE surface as a result of the relatively greater equilibrium shift in that direction.

Figure 4A shows how current response in the CVs varied as a function of APAP concentration from 0.5 to  $13.0 \text{ mmol dm}^{-3}$ . Figure 4B shows a correlation between the peak current and the concentration of APAP ( $\text{mmol dm}^{-3}$ ) at the reduction potential of  $-0.058 \text{ V}$  (dash dot red line) according to the equation:

$$I_p (\mu\text{A}) = (1.518) [\text{APAP}] + 2.814 \quad (R^2 = 0.9663) \quad (4)$$

Likewise, Figure 4B also demonstrates a correlation between peak current and APAP concentration at oxidation potential of  $+0.568 \text{ V}$  (solid black line), according to the equation:

$$I_p (\mu\text{A}) = (8.392)[\text{APAP}] + 6.714 \quad (R^2 = 0.9732) \quad (5)$$

The SiNWs demonstrated excellent sensing capabilities towards APAP at an oxidation potential of  $+0.568 \text{ V}$  as shown by CA (Figure 5A). It was determined that APAP can be detected at concentrations as low as  $0.01 \text{ mmol dm}^{-3}$ . The GCE modified by SiNWs showed a clear increase in current with increasing APAP concentrations. The detection limit was found to be  $0.05 \text{ mmol dm}^{-3}$  (equivalent to  $7.558 \mu\text{g/mL}$ ). Figure 5A (the plot of peak current versus APAP concentration in inset) shows a linear relationship with correlation coefficient  $R^2=0.9694$  for APAP concentrations from 0.01 to  $3 \text{ mmol dm}^{-3}$ . Therapeutic levels of APAP are within the concentration range of 0.06 to  $0.16 \text{ mmol dm}^{-3}$  (10 to  $25 \mu\text{g/mL}$ ) [7]. An improved correlation coefficient of  $R^2=0.9900$  is observed in this range (Figure 5B). Selectiv-

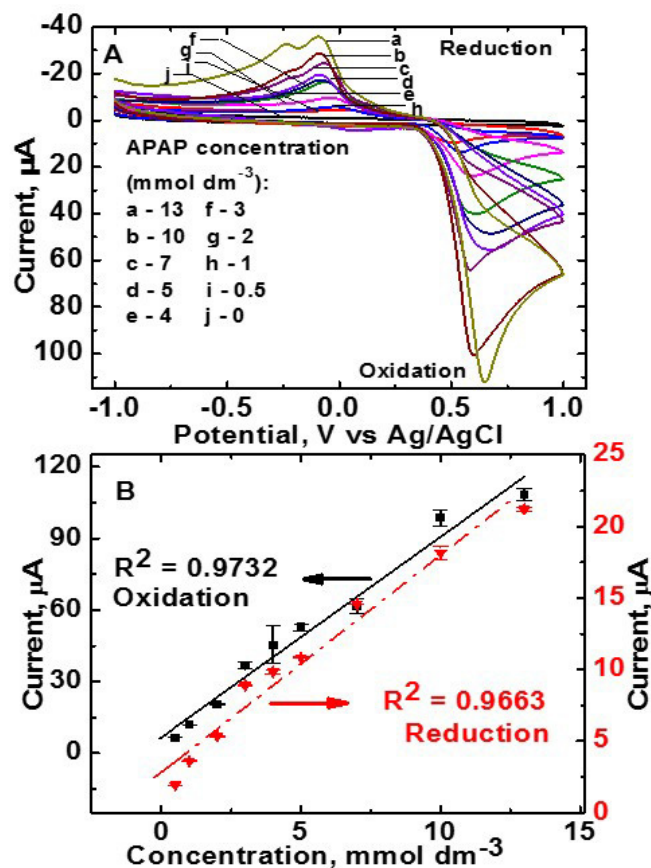


Fig. 4. (A) CV for the effect of concentration of APAP in  $70 \text{ mmol dm}^{-3}$  PBS at  $\text{pH}=7.4$  with a  $50 \text{ mV s}^{-1}$  scan rate. (B) Calibration curve of modified GCE current vs concentration under oxidation (solid black line, left y-axis) and reduction (dash dot red line, right y-axis) potentials.

ity of the Nafion/SiNW/GCE sensor towards APAP was examined in the presence of the following clinically relevant interfering analytes: glucose (Glu), ascorbic acid (AA), hydrogen peroxide ( $\text{H}_2\text{O}_2$ ), folic acid (FA), and uric acid (UA). Figure 6 shows the chronoamperometric responses of the Nafion/SiNW/GCE at  $+0.568 \text{ V}$  (APAP's determined oxidation potential) versus Ag/AgCl upon sequential additions of  $1 \text{ mmol dm}^{-3}$  APAP, Glu, AA,  $\text{H}_2\text{O}_2$ , FA, UA, and APAP. These species were added at various time points, denoted by the arrows in Figure 6. Nafion/SiNW/GCE could selectively detect APAP in the presence of all of these potentially interfering species. No detectable current response is observed, showing that the SiNW electrochemical cell is selective to only APAP.

#### 4 Conclusions

GCEs modified with SiNWs have demonstrated selective and sensitive electrochemical detection of APAP. CVs of the SiNWs in the  $0.5$  to  $13 \text{ mmol dm}^{-3}$  APAP concentration range allowed for the determination of the APAP oxidation and reduction potentials. Electrocatalytic activ-

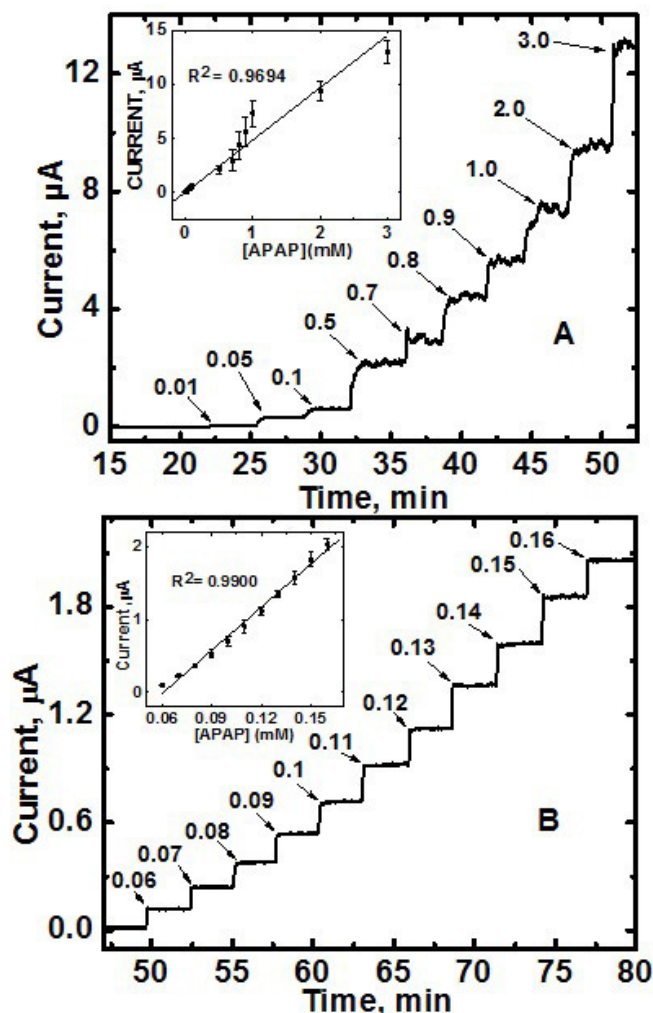


Fig. 5. (A) CA response of Nafion/SiNW/GCE in PBS,  $\text{pH}=7.4$ , after increasing the APAP concentration from  $0.01$  to  $3 \text{ mmol dm}^{-3}$  (denoted with arrows in the plot) at  $+0.568 \text{ V}$  with the calibration curve of current vs concentration in the inset. (B) CA response of Nafion/SiNW/GCE in PBS,  $\text{pH}=7.4$  from  $0.06$  to  $0.16 \text{ mmol dm}^{-3}$  indicated by arrows in the plot at  $+0.568 \text{ V}$  with the inset of calibration curve of current vs concentration.

ity was higher in oxidation compared to that of reduction, owing to differences in diffusion coefficients. The SiNWs demonstrated a clear increase in current with increase in APAP concentrations in the  $0.01$  to  $3 \text{ mmol dm}^{-3}$  range with excellent linearity within the  $0.06$  to  $0.16 \text{ mmol dm}^{-3}$  range in the CA analysis. SiNWs were highly selective to APAP in the presence of an array of interfering analytes (UA, FA, Glu, AA, and  $\text{H}_2\text{O}_2$ ) with sufficient sensitivity to detect APAP at concentrations from  $0.01$  to  $3 \text{ mmol dm}^{-3}$  in PBS ( $\text{pH}=7.4$ ), hence demonstrating promise for practical clinical APAP monitoring.

#### Acknowledgements

We gratefully acknowledge support of this work from the Faculty Research and Creative Activity Committee

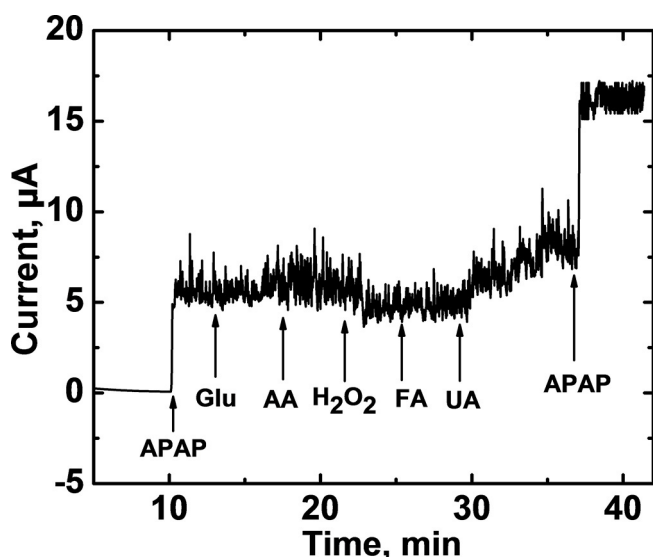


Fig. 6. CA response of Nafion/SiNW/GCE at +0.568 V vs Ag/AgCl to the sequential addition of 1 mmoldm<sup>-3</sup> APAP, Glu, AA, H<sub>2</sub>O<sub>2</sub>, FA, UA, and APAP in pH=7.4 PBS.

(FRCAC) of Middle Tennessee State University (MTSU). We are also grateful to Ms. Joyce Miller of the MTSU Interdisciplinary Microanalysis and Imaging Center (MIMIC) for assistance in obtaining the SEM and EDX images of the SiNWs used in this study. S.K. acknowledges support from the U.S. Department of Commerce, National Institute of Standards and Technology under the financial assistance award 70NANB16H043.

## References

- [1] T. S. Chen, K. L. Huang, *Int. J. Electrochem. Sci.* **2012**, *7*, 6877–6892.
- [2] K. Choi, Y. Kim, J. Park, C. K. Park, M. Y. Kim, P. Kim, *Sci. Total Environ.* **2008**, *405*, 120–128.
- [3] R. Andreozzi, M. Raffaele, P. Nicklas, *Chemosphere* **2003**, *50*, 1319–1330.
- [4] H. Nakata, K. Kannan, P. D. Jones, J. P. Giesy, *Chemosphere* **2005**, *58*, 759–766.
- [5] K. D. Brown, J. Kulis, B. Thomson, T. H. Chapman, D. B. Mawhinney, *Sci. Total Environ.* **2006**, *366*, 772–783.
- [6] R. J. Fontana, *Med. Clin. North Am.* **2008**, *92*, 761–794.
- [7] E. L. Brandwene, S. R. Williams, C. Tunget-Johnson, S. G. Turchen, A. S. Manoguerra, R. F. Clark, *J. Emerg. Med.* **1996**, *14*, 691–695.
- [8] M. E. Bosch, A. J. R. Sanchez, F. S. Rojas, C. B. Ojeda, *J. Pharm. Biomed. Anal.* **2006**, *42*, 291–321.
- [9] S. A. Kumar, C. F. Tang, S. M. Chen, *Talanta* **2008**, *76*, 997–1005.
- [10] A. M. Morales, C. M. Lieber, *Science* **1998**, *279*, 208–211.
- [11] Y. F. Zhang, Y. H. Tang, N. Wang, D. P. Yu, C. S. Lee, I. Bello, S. T. Lee, *Appl. Phys. Lett.* **1998**, *72*, 1835–1837.
- [12] S. Krylyuk, A. V. Davydov, I. Levin, *ACS Nano* **2011**, *5*, 656–664.
- [13] J. A. Martinez, N. Misra, Y. Wang, P. Stroeve, C. P. Grigoropoulos, A. Noy, *Nano Lett.* **2009**, *9*, 1121–1126.
- [14] G. Zheng, F. Patolsky, Y. Cui, W. U. Wang, C. M. Lieber, *Nat. Biotechnol.* **2005**, *23*, 1294–1301.
- [15] D. K. Nagesha, M. A. Whitehead, J. L. Coffey, *Adv. Mater.* **2005**, *17*, 921–924.
- [16] Y. Cui, Q. Wei, H. Park, C. M. Lieber, *Science* **2001**, *293*, 1289–1292.
- [17] Z. Li, Y. Chen, X. Lee, T. I. Kamins, K. Nauka, R. S. Williams, *Nano Lett.* **2004**, *4*, 245–247.
- [18] Z. Guo, M. L. Seol, C. Gao, M. S. Kim, J. H. Ahn, Y. K. Choi, X. J. Huang, *Electrochim. Acta* **2016**, *211*, 998–1005.
- [19] V. Krivitsky, M. Zverzhinetsky, F. Patolsky, *Nano Lett.* **2016**, *16*, 6272–6281.
- [20] D. Nematollahi, H. Shayani-Jam, M. Alimoradi, S. Niroormand, *Electrochim. Acta* **2009**, *54*, 7407.
- [21] R. Zahn, G. Coullerez, J. Voros, T. Zambelli, *J. Mater. Chem.* **2012**, *22*, 11073–11078.
- [22] A. J. Bard, L. R. Faulker, *Electrochemical Methods: Fundamentals and Applications*. Wiley, New York, **2001**.
- [23] A. C. F. Ribeiro, M. C. F. Barros, L. M. P. Verissimo, C. I. A. V. Santos, A. M. T. D. P. V. Cabral, G. D. Gaspar, M. A. Estes, *J. Chem. Thermodyn.* **2012**, *54*, 97–99.
- [24] J. P. Cloarec, C. Chevalier, J. Genest, J. Beauvais, H. Chamas, Y. Chevolut, T. Baron, A. Souifi, *Nanotechnol.* **2016**, *27*, 1–9.

Received: December 6, 2017

Accepted: January 26, 2018

Published online on February 8, 2018

## Supporting Information

### Electrochemical Detection of Acetaminophen Using Silicon Nanowires

Raja Ram Pandey<sup>1</sup>, Hussain S. Alshahrani,<sup>1</sup> Sergiy Krylyuk,<sup>2,3</sup> Elissa H. Williams,<sup>3</sup> Albert V. Davydov,<sup>3</sup> and Charles C. Chusuei<sup>1,\*</sup>

<sup>1</sup>Chemistry Department, 440 Friendship Street, Middle Tennessee State University, Murfreesboro, TN 37132, USA

<sup>2</sup>Theiss Research, La Jolla, CA 92037, USA

<sup>3</sup>Materials Science and Engineering Division, Material Measurement Laboratory, National Institute of Standards and Technology, Gaithersburg, MD 20899, USA

#### 1. Surface Characterization by SEM, EDX, ATR-IR, and XPS

Scanning electron micrographs (SEMs) of the SiNWs were used to quantify the surface density of material deposited onto the electrodes for electrochemical analysis. SEM analysis was performed using a Hitachi S3400N SEM operated at 15 kV with 18,000x magnification. **Figure S1** shows a representative SEM image of the rod-shaped SiNWs.

Energy dispersive X-ray (EDX) spectroscopy of the SiNWs was used to analyze the elemental composition present in the composite. EDX analysis was performed using Oxford Inca X-act instrument. **Figure S2** shows the SEM image of the SiNWs accompanying the EDX data, indicating Si and O present on the GCE surface. EDX scans of the SiNWs deposited on the electrode surface had an average atomic percent composition of  $66 \pm 8\%$  O and  $34 \pm 8\%$  Si from  $n = 6$  samplings.

ATR-IR analysis was carried out using a Varian 7000 FTIR with a mercury cadmium telluride (MCT) detector and Varian Resolution Pro software, ver. 5.0 (Randolph, MA, USA). The detector was cooled with liquid nitrogen (LN<sub>2</sub>) and data was obtained after a 30 min equilibration time. Air was used for background subtraction. A Golden Gate ATR diamond crystal was used as the support in the instrument's sample compartment. ATR-IR spectra of SiNWs is shown in **Figure S3** along with that of isopropanol (background solvent). The two peaks with asterisk signs at 1546 and 1742 cm<sup>-1</sup> are attributed to the SiCH=CH<sub>3</sub> and SiO-C-OCH<sub>3</sub> vibrations [1], respectively. Other peaks are attributed to artifacts from isopropanol in which SiNWs were

dispersed. The spectrum of SiNWs was obtained after depositing and drying 600  $\mu\text{L}$  of SiNWs solution on the crystal of the ATR-IR instrument.

XPS measurements were performed using a Perkin Elmer PHI 560 instrument with a 25-270AR double-pass cylindrical mirror analyzer operated at 12 kV and 225 W with a Mg K $\alpha$  anode using a photon energy of  $h\nu = 1253.6$  eV. A binding energy (BE) of 284.7 eV for the C 1s orbital, denoting adventitious carbon [2], was used for charge referencing. Shirley background subtractions for Si 2p and O 1s peaks were used. Deconvolutions were performed using a 70 % to 30 % Gaussian-Lorentzian line-shape with the assistance of CasaXPS software, version 2.2.107 (Devon, United Kingdom). To perform the scans, a Si (100) wafer containing the SiNWs was mounted onto the XPS sample holder, and outgassed in a turbo-pumped antechamber. The system pressure did not exceed  $1.0 \times 10^{-8}$  Torr during XPS analysis. XPS high resolution narrow scans for O 1s, C 1s and Si 2p were carried out. Atomic percent composition measured from the C 1s, O 1s and Si 2p orbitals, after normalizing their integrated peak areas to their atomic sensitivity factors [3], were 19.4 %, 74.0 % and 6.5 %, respectively. **Figure S4 (A)** presents the O 1s XPS spectrum for SiNWs. XPS spectra of O 1s orbitals for the SiNWs was curvefitted using the same BE positions and line-shapes for SiNWs reported by Lamaa et al. [4] for reference positions (**Figure S4A**). BE peak centers (with full-width-at-half-maxima in parentheses) were fixed at 531.6 (2.0) and 532.7 (2.0) eV, denoting SiO<sub>2</sub> and adsorbed hydroxyls, respectively. **Figure S4 (B)** displays the XPS spectrum of silicon which provides two Si 2p peaks at 103.0 (2.3) eV and 99.1 (1.8) eV related to silicon oxide and silicon, respectively.

## 2. Optimum SiNW Loading Density

**Figure S5 (A)** shows CV responses determined using various SiNWs loadings. **Figure S5 (B)** demonstrates that both cathodic (reduction) and anodic (oxidation) currents are highest at a 20- $\mu\text{L}$  loading corresponding to approximately  $1.4 (\pm 0.5) \times 10^3$  SiNWs/ $\text{mm}^2$  based on an average of  $n = 53$  SEM images. The SiNWs were applied to the GCE surface using droplets corresponding to an estimated  $7 \times 10^2$  SiNWs per 10- $\mu\text{L}$  droplet applied in each application. SiNW loadings above or below the 20- $\mu\text{L}$  aliquot total volume resulted in reduced current observed for APAP detection.

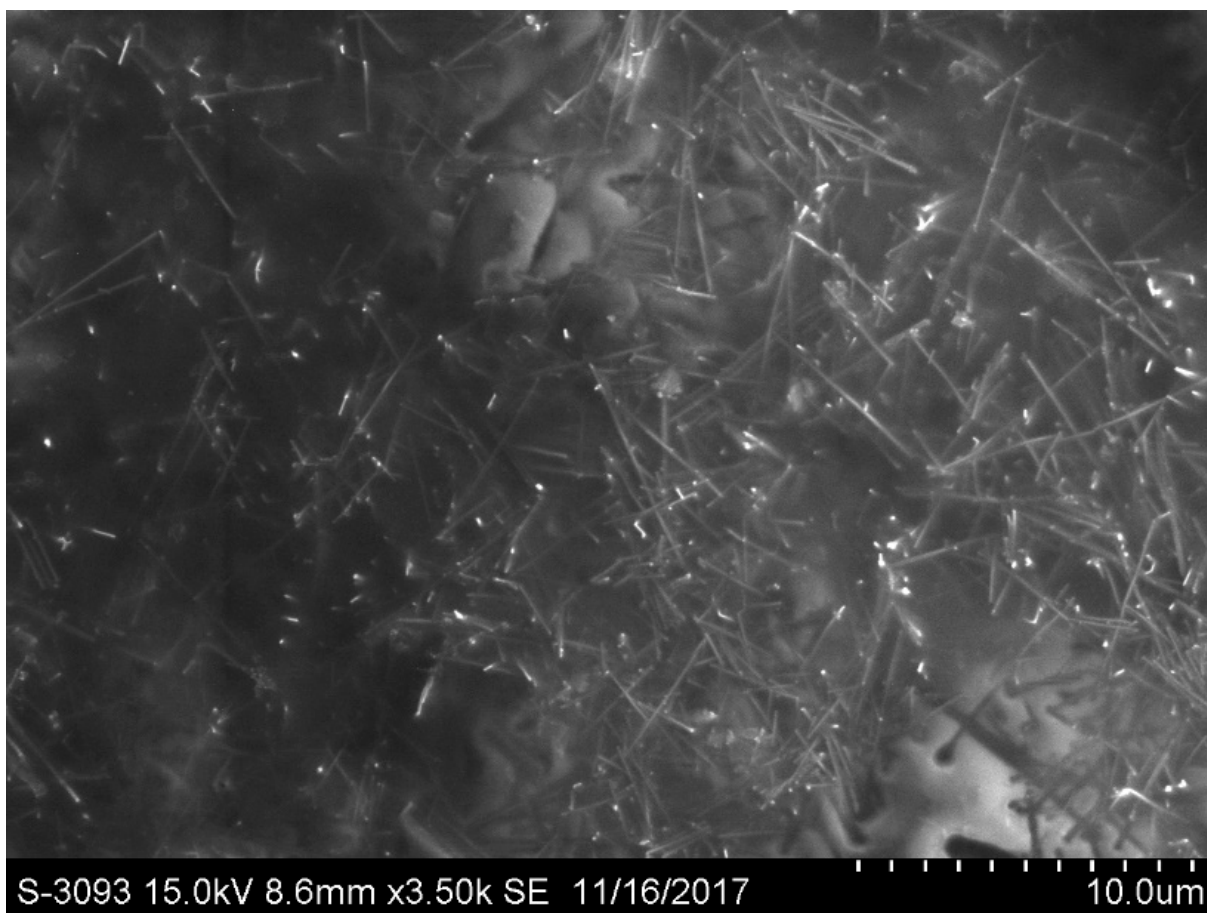


**Figure S1.** Representative SEM of 30 nm diam SiNWs deposited on the GCE after sonication.

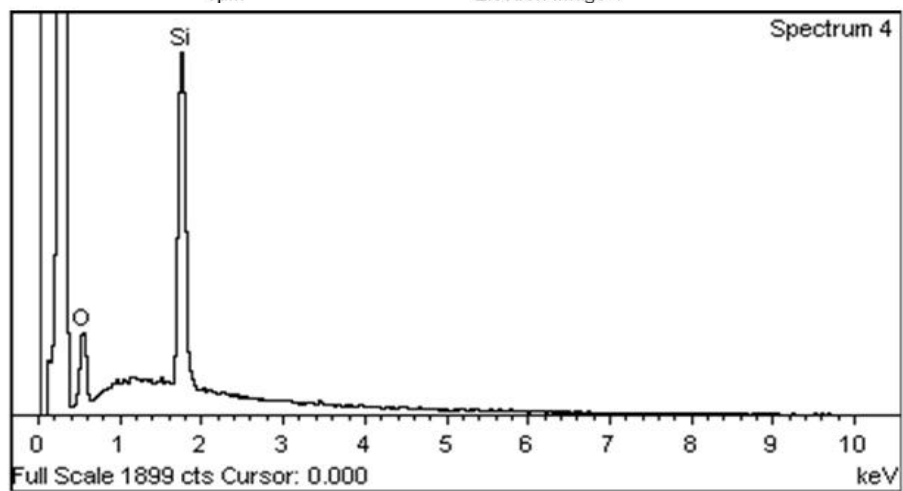
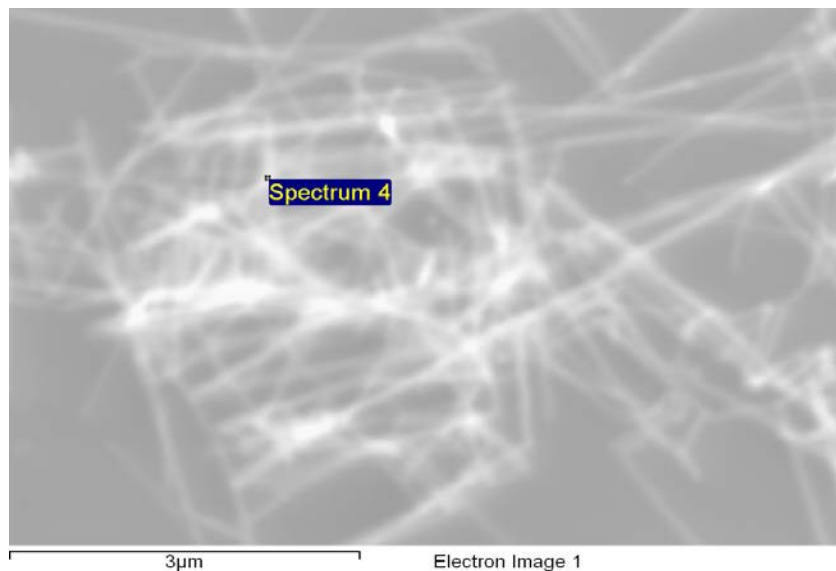


**Figure S2.** EDX image and spectrum of 30 nm diam SiNWs on GCE.

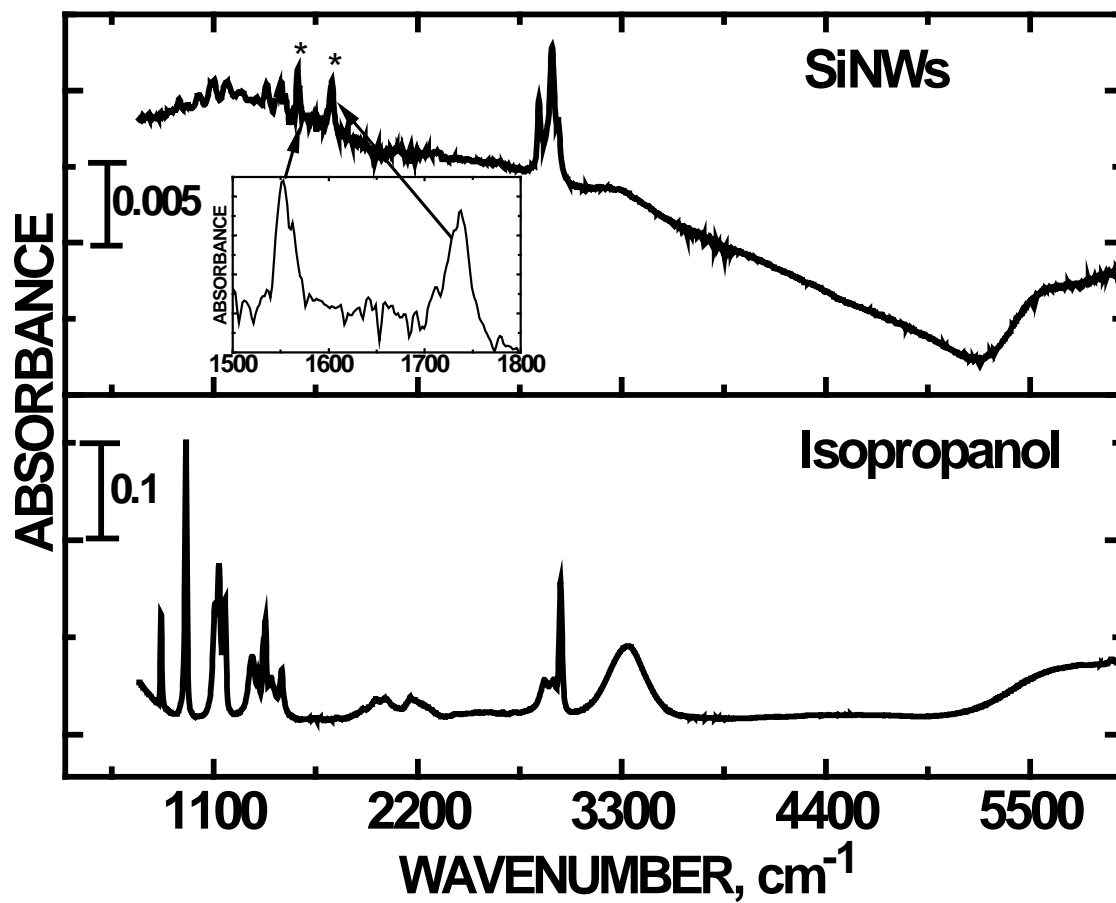


**Figure S3.** ATR-IR spectra of SiNWs (top) and isopropanol (bottom) along with inset showing the expanded form of the two peaks (in asterisks) attributed to SiNWs.

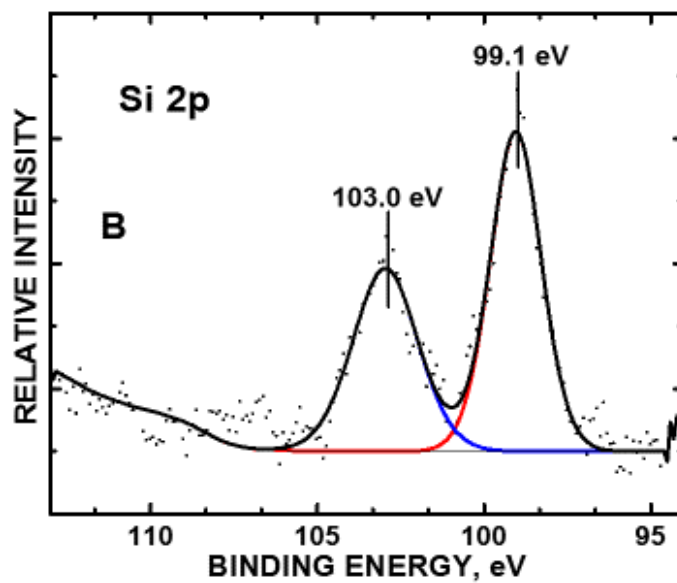
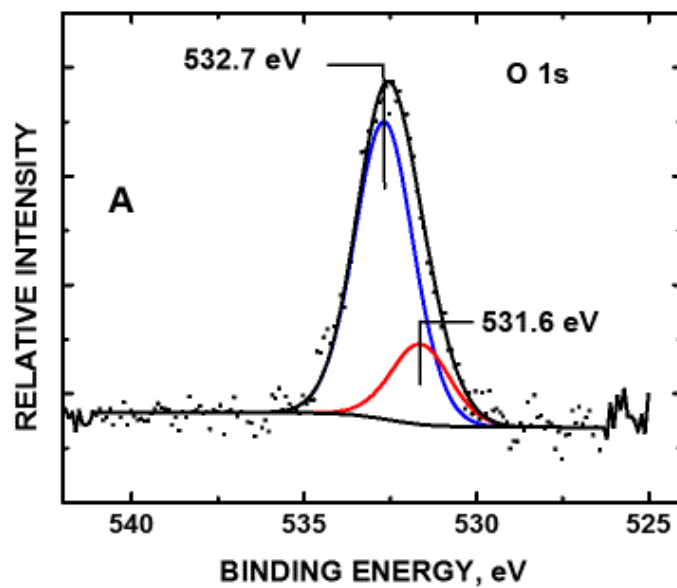


**Figure S4.** XPS narrow scans of the (A) O 1s, and (B) Si 2p core orbitals of SiNWs.

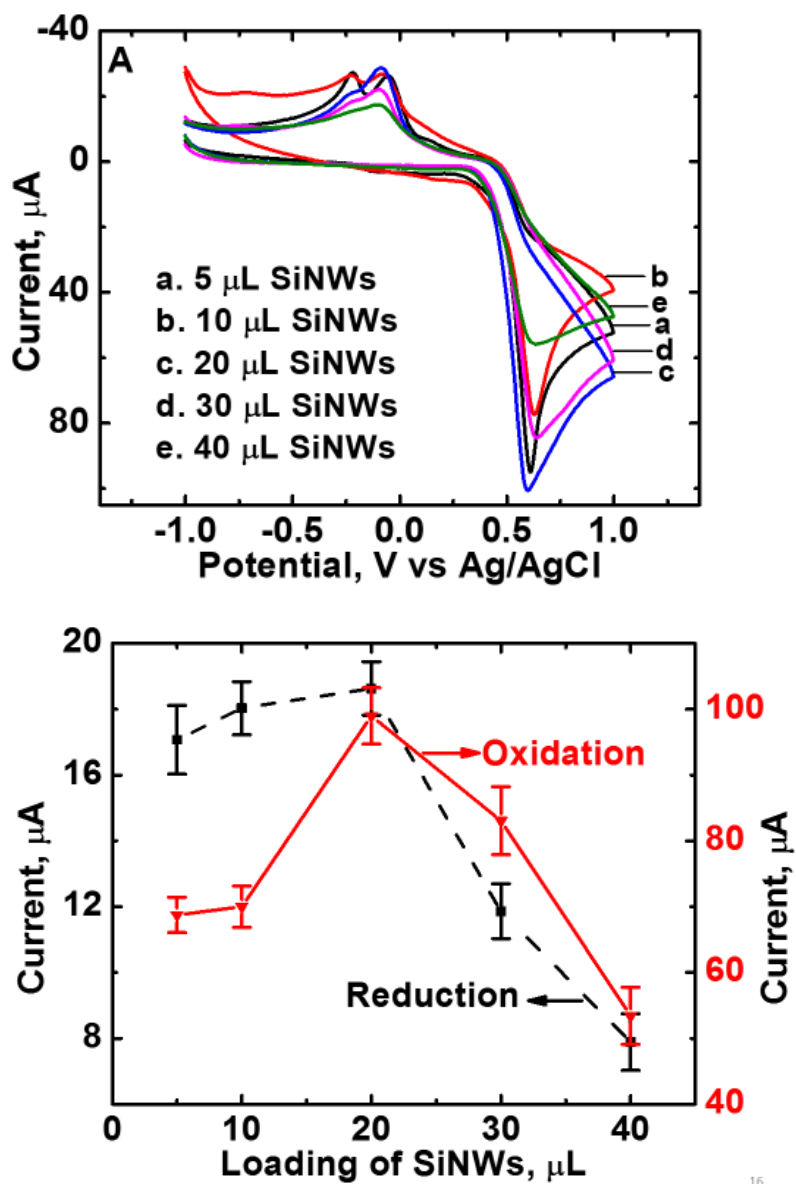


**Figure S5.** (A) CVs of Nafion/SiNW/GCE in 10 mmol dm<sup>-3</sup> APAP at pH = 7.4 with different loadings of SiNWs at 50 mV s<sup>-1</sup> scan rate. (B) Reduction and oxidation peak current vs SiNW loading.

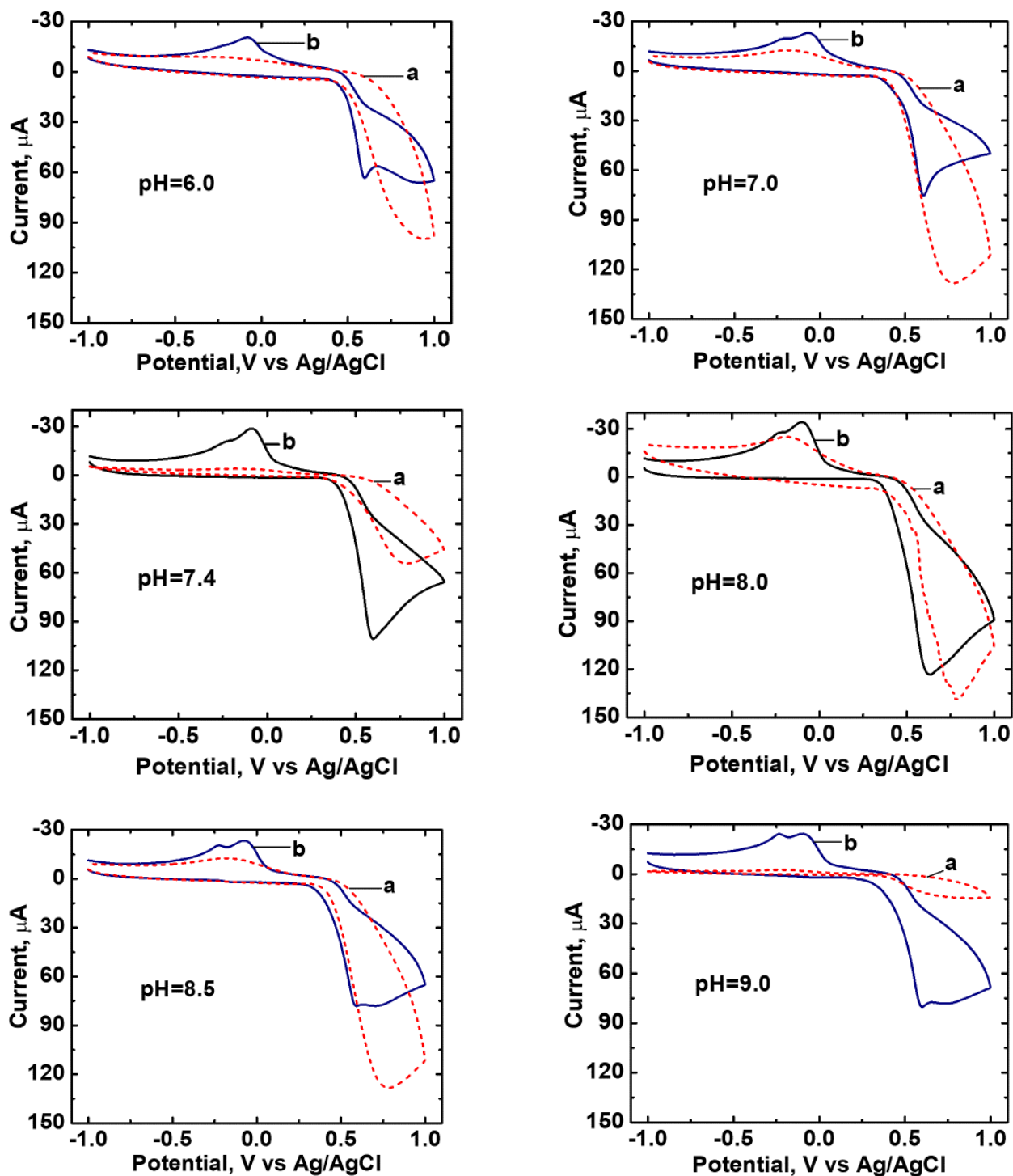


**Figure S6.** CVs of (a) bare GCE and (b) Nafion/SiNWs/GCE in  $10 \text{ mmol dm}^{-3}$  APAP in  $\text{N}_2$ -saturated phosphate buffer with pH = 6.0 to 9.0 at a scan rate of  $50 \text{ mV s}^{-1}$ .

## References

- [1] A. L. Smith, *Applied Infrared Spectroscopy*, Wiley and Sons: New York, 1979.
- [2] T. L. Barr, S. Seal, Nature of the use of adventitious carbon as a binding energy standard. *J. Vac. Sci. Technol. A* **1995**, 13, 1239-1246.
- [3] C. D. Wagner, L. E. Davis, M. V. Zeller, J. A. Taylor, R. H. Raymond, L. H. Gale, Empirical atomic sensitivity factors for quantitative analysis by electron spectroscopy for chemical analysis. *Surf. Interface Anal.* **1981**, 3, 211-225.
- [4] L. Lamaa, C. Ferronato, S. Prakash, L. Fine, F. Jaber, J. M. Chovelon, Photocatalytic oxidation of octamethyl cyclotetrasiloxane (D<sub>4</sub>): Towards a better understanding of the impact of volatile methyl siloxanes on photocatalytic systems. *Appl. Catal. B: Environ* **2014**, 156, 438-446.

**Table S1. Calculation of Diffusion Coefficients**

F	96485.3329 C	$I_p = 0.4961 \text{ nFA } C_o^* \left( \frac{\alpha n F v D_E}{RT} \right)^{1/2}$
R	8.314 J mol <sup>-1</sup> K <sup>-1</sup>	
T	295.15 K	Using this equation, $\alpha D$ was calculated as
n	2	
A	0.19625 cm <sup>2</sup>	$\alpha D_E = \frac{(I_p)^2 RT}{nF(\sqrt{v})^2 (0.4961 nFA C_o^*)^2}$
$C_o^*$	0.00001 moles cm <sup>-3</sup>	
constant	0.4961	

For oxidation:

$v^{1/2}$ (V)	$i_{pa}$ (A)	$\alpha D$ ( cm <sup>2</sup> s <sup>-1</sup> )	
0.00316	3.199E-05	3.692E-05	
0.00447	3.586E-05	2.319E-05	
0.00547	3.967E-05	1.895E-05	
0.00632	4.284E-05	1.656E-05	
0.00707	4.650E-05	1.558E-05	
0.00774	4.989E-05	1.497E-05	
0.00836	5.258E-05	1.425E-05	
0.00894	5.517E-05	1.372E-05	
0.00948	5.774E-05	1.336E-05	
0.01000	5.975E-05	1.286E-05	
0.01048	6.401E-05	1.344E-05	STD
	average =	<b>1.762E-05</b>	7.09E-06

For reduction :

$v^{1/2}$ (V)	$i_{pa}$ (A)	$\alpha D$ ( cm <sup>2</sup> s <sup>-1</sup> )	
0.00316	5.000E-06	9.019E-07	
0.00447	8.002E-06	1.155E-06	
0.00547	9.502E-06	1.087E-06	
0.00632	9.991E-06	9.002E-07	
0.00707	1.049E-05	7.931E-07	
0.00774	1.199E-05	8.650E-07	
0.00836	1.262E-05	8.212E-07	
0.00894	1.348E-05	8.189E-07	
0.00948	1.419E-05	8.073E-07	
0.01000	1.514E-05	8.260E-07	
0.01048	1.639E-05	8.812E-07	STD
	average =	<b>8.960E-07</b>	1.18E-07